# Fast and robust *dq* voltage controller for a three-phase four-leg inverter operating in an islanded microgrid

Mohammad Reza Miveh
Department of Electrical Engineering,
Tafresh University, Tafresh, 39518-79611, Iran

Shahrokh Akhlaghi
Electrical and Computer Engineering Department,
Binghamton University, Binghamton, NY 13902, USA

Mojtaba Pishvaee
Department of Electrical Engineering,
Tafresh University, Tafresh, 39518-79611, Iran

Ali Asghar Ghadimi
Electrical Engineering Department,
Faculty of Engineering, Arak University, Arak, Iran

Saleh Saeidi
Department of Electrical Engineering,
Islamic Azad University, Arak Branch, Arak, Iran

***Abstract*— This paper suggests a fast and robust *dq* voltage control strategy for a three-phase four-leg voltage source inverter (VSI) operating with highly unbalanced loads in a stand-alone distribution network. The main objective is to balance the output voltages of the four-leg inverter under unbalanced load conditions with fast transient response. The proposed control strategy consists of a proportional-integral (PI) voltage controller and a proportional current loop in each phase. The voltage controller and the current control loop are, respectively, used to regulate the instantaneous output voltage and generate the pulse width modulation (PWM) voltage command with fast transient response. A voltage decoupling feedforward path is also used to improve the system robustness. Simulation results are also carried out using the DIgSILENT PowerFactory software to verify the effectiveness of the suggested control strategy.**

***Keywords*—Four-leg inverter; microgrid; voltage source inverter (VSI); four-wire system; unbalanced load.***

## I. INTRODUCTION

Small autonomic grids have been in existence in remote communities for many decades [1]. For economic and technical reasons, the interconnection of these remote grids is not feasible with the public grid. Over the last decades, due to the availability of fossil-fuels to generate huge amounts of electricity, there has been a general trend towards using such kind of energies [2]. Nonetheless, with the emergence of renewable and sustainable energies, integrating such technologies has become a priority in this distribution network.

In order to efficiently share green energies into small autonomic grids, numerous technical issues should be addressed. Indeed, not only the potential advantages of renewable energy should be harnessed, but also the present levels of reliability, power quality and controllability must be maintained [3]. The emergence of microgrid is a reasonably attractive alternative for overcoming the challenges of integrating distributed energy resources (DERs) into the active distribution networks [4].

Islanded microgrids can be defined as a cluster of distributed generations (DGs), loads, power electronic devices and energy storage systems, which connected through arelatively small grid at low voltage levels [5-7]. Power electronic devices are widely utilized in energy storage systems and DGs to convert power from a direct current (DC) to an appropriate alternating current (AC) form. These DC/AC power cconverters can be operated in two modes, including grid-feeding mode and grid-forming mode [8]. In grid-forming mode, the power converter is responsible for regulating the output voltage and frequency of an inverter-based DER in the islanded mode. In this strategy, the DER acts as a Voltage Source Inverter (VSIs) [9]. This DER is called the grid-forming unit because it is responsible for forming the microgrid bus voltage in the island mode. When a single DER is responsible for controlling the voltage and frequency, the microgrid is called a single-master microgrid [9].

On the other hand, the main aim of the primary controller, in grid-feeding mode, is to regulate the active and reactive power of DERs at certain references [10]. This strategy assumes that the microgrid is formed by another grid-forming unit or units, and the grid-feeding unit is designed to deliver the desired active and reactive power to this energized grid [11]. In other words, the grid-feeding power converter cannot form an island microgrid [12]. In summary, the previously mentioned primary control schemes are the main approaches to form a microgrid. The choice of a suitable control strategy is mainly based on the characteristics of the primary source and the desired role of that source in the microgrid system.

In many microgrids, electrical power is distributed through a three-phase four-wire system. In some circumstance, the VSIs used in islanded mode must be supplied unbalanced loads. The increasing presence of single-phase loads and generators in three-phase four-wire microgrids may lead to unbalance of the three-phase voltages. Unbalanced loads may affect the proper function of autonomous microgrids. Malfunction of protection devices and adjustable speed drives, losses in rotating machines and saturation of transformers are the main challenges caused by unbalanced loads. Hence, it is important to propose a suitable control strategy for inverter-based DGs in microgrids to operate under unbalanced load conditions without any performance degradations.

In recent years, a considerable amount of literature has been published on the control of four-leg VSIs in stand-alone mode [12-24]. They include the following: hysteresis controllers [12], proportional-integral (PR) controllers [13-17], controllers based on symmetrical components calculators (SCCs) [18-20], predictive controllers [21-23] and sliding mode controllers [24]. However, these control techniques often suffer from slow transient response, complex control algorithm, and unsatisfactory steady-state voltage tracking error.

In this paper, a fast and robust *dq* voltage controller strategy for a four-leg grid-forming power converter is presented. The main aim is to efficiently balance the output voltages of the four-leg inverter under unbalanced load conditions. Simulation results are provided to confirm the effectiveness of the proposed control scheme.

The rest of this paper is organized as follows. Section 2 describes the model of the four-leg inverter. Section 3 presents the proposed per-phase multi-loop control of the four-leg inverter in the dq frame. Simulation results are provided in section 4. Finally, the conclusion gives a brief summary and critique of the findings.

## II. SYSTEM MODELING

Fig. 1 shows the power stage of a four-leg grid-forming inverter and its LC output filter connected to unbalanced loads. It is worth noting that the neutral line of the four-wire system is provided by connecting the fourth leg of the four-leg inverter to the neutral point of loads. The additional leg regulates the load zero sequence voltage. To minimize the switching frequency ripple imposed on the neutral current inverter ($i_n$), a neutral inductor ($L_n$) is also used.

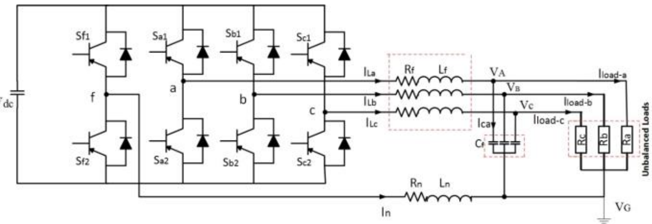

Fig. 1. Power stage of a three-phase four-leg VSI.

The carrier-based pulse width modulation (PWM) technique is selected to produce three output voltages independently because of its simplicity and ease of implementation. Table I presents the parameters of the four-leg VSI. To describe the behavior of the circuit depicted in Fig. 1, the following quantities for voltages and currents can be defined:

$$V_{pwm}=[v_{af} \quad v_{bf} \quad v_{cf}]^T \tag{1}$$

where $V_{pwm}$ is the vector of three-phase inverter output line-to-neutral PWM voltages.

$$I_{inv}=[I_{la} \quad I_{lb} \quad I_{lc}]^T \tag{2}$$

$$I_{load}=[I_{load-a} \quad I_{load-b} \quad I_{load-c}]^T \tag{3}$$

$$V_{load}= [V_A \quad V_B \quad V_C]^T \tag{4}$$

By applying Kirchhoff voltage and current laws to the power stage of the three-phase four-leg VSI, the following equations can be obtained.

TABLE I. SYSTEM PARAMETERS.

| Parameter | Description | Value |
|---|---|---|
| $f_s$ | switching frequency | 5 kHz |
| $w_f$ | fundamental frequency | $2\pi 60$ rad/s |
| $L_f$ and $L_n$ | filter inductance | 0.1 mH |
| $C_f$ | filter capacitance | 300 $\mu F$ |
| $R_f$ and $R_n$ | resistor of the filter inductance | 10 mΩ |
| $V_{dc}$ | DC-link voltage | 300 V |

$$V_{load} = R_f I_{inv} + L_f \frac{dI_{inv}}{dt} + V_{pwm} - R_n i_n - L_n \frac{di_n}{dt}. \tag{5}$$

$$\dot{I}_{inv} = I_{load} + C_f \frac{dV_{load}}{dt}. \tag{6}$$

The control system tuning and stability analysis of the four-leg inverter can be performed on a per-phase basis. Hence, the power stage of the four-leg inverter is modeled according to the principles of the per-phase basis so that only a single-phase representation of the inverter is used for the analysis and design. Fig. 2 illustrates the per-phase representation of the four-leg inverter for one phase to neutral connection. As can be seen, the fundamental component of the switched voltage of each phase and the connected load to that phase are modeled as an ideal controlled voltage source ($uV_{dc}$, which $u$ is the control variable) and a current source ($I_o$), respectively. In this Figure, $i_L$ and $v_c$ are also the respective phase inductor current and capacitor voltage, respectively.

For implementation of a single-phase system in the synchronous reference frame, it is necessary to generate a pseudo-two-phase system. In this two-phase system, one component is obtained from the original single-phase system ($\alpha$) and an orthogonal signal ($\beta$) must be created from the original single-phase signal. Based on the Fig. 2, the differential equations representing the model of the single-phase system in the $\alpha\beta$ frame can be written as:

$$L\frac{di_{l,\alpha\beta}}{dt} = uV_{dc,\alpha\beta} - v_{c,\alpha\beta} - Ri_{l,\alpha\beta} \tag{7}$$

$$C\frac{dv_{c,\alpha\beta}}{dt} = i_{l,\alpha\beta} - i_{o,\alpha\beta} \tag{8}$$

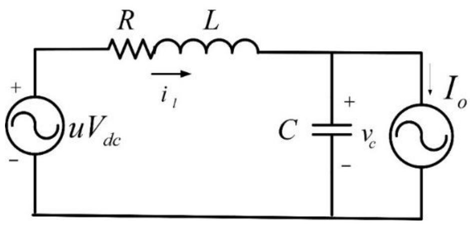


Fig. 2. Basic per-phase representation of the four-leg inverter in each phase.

The average switching model of the four-leg VSI in each phase is depicted in Fig. 3. This is obtained by assuming that the switching frequency is much higher than the fundamental frequency. As can be seen from the Fig. 3, $\tilde{m}$(the function of modulating signal) is used instead of the control variable, which represents the average value of $u$ over one cycle of switching frequency.

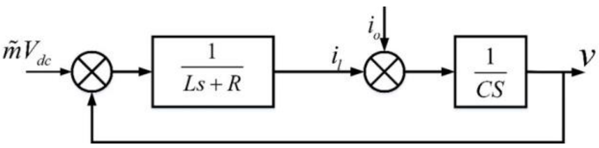


Fig. 3. Average switching model of the four-leg VSI in each phase.

## III. Suggested Control Scheme

The implementation of the independent control of the single-phase system in the dq frame needs to create a secondary orthogonal signal from each original phase signal through a complex orthogonal signal generation (OSG) technique. Several attempts have been made in the literature to generate an orthogonal signal from an original single-phase signal such as second-order generalized integrator, Kalman filter and first-order all-pass filter (APF) methods [25]. In this paper, the orthogonal signal is generated based on the reference values of the d and q-axes. The proposed method exhibits improved steady-state and dynamic performances in comparison with the inverters equipped with the conventional orthogonal signal generation techniques.

The structure of the suggested control scheme for phase ‘a’ is presented in Fig. 4. The control system consists of an inner current loop and an outer voltage loop in each phase. The main function of the external voltage loop is to control the instantaneous output voltages within the standard limits. The inner current loop is also adopted to generate the switching states of the PWM modulator. In addition, it improves the transient performance of the proposed control scheme. A voltage decoupling feedforward ($v^*$) is also used to enhance the control system robustness. It is noteworthy that the capacitor current is employed as the feedback signal in the inner loop due to its superior performance in rejecting disturbances rather than the inductor current. Furthermore, the use of the capacitor current is much easier and more cost-effective than the inductor current. According to the basic principles of control theory of cascaded control, these loops can be designed independently as long as the dynamics of the voltage loop is designed to be slower than the internal current controller.

The voltage loop operates in the synchronous reference frame, whereas the inner current loop functions in the stationary coordinate system. In the outer loop, $V_{ca}$ is the a-phase output voltage of the filter capacitor to the neutral line. $V_\alpha$ and $V_\beta$ are the real and the orthogonal components of the $V_{ca}$ in the stationary reference frame, respectively. The dq components of the a-phase output voltage of the filter capacitor can be generated by applying the Park transformation, after creating the pseudo-two-phase system. A simple phase locked loop (PLL) is used to obtain the $\sin\theta$ and $\cos\theta$ terms. The PI controllers are utilized in the voltage loop to regulate the instantaneous output voltages in the dq frame. The reference voltages for the three phases have equal amplitudes, but are separated from the other voltages by a phase angle of 120°. The q-component of the reference voltages in each phase ($V_q^*$) is set at 0, whereas the d-components ($V_d^*$) is set at the peak value of the reference phase voltage.

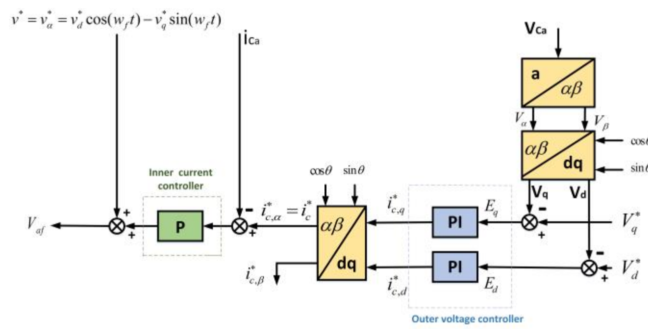


Fig. 4. Per-phase cascaded controller for the four-leg inverter in phase ‘a’.

The reference signal of the internal current loop is provided by employing the inverse Park transformation to the output signals of the output voltage controller. As shown in Fig. 4, only the $\alpha$-axis quantity generated by the outer voltage loop is fed to the internal current controller for compensation. It is the real signal of the two-phase system. Afterwards, the inner loop generates the switching states of the PWM using a simple proportional controller. The parameters of the controller are obtained from a step-by-step systematic design procedure [19].

## IV. Simulation Results

To validate the performance of the proposed control strategy, the test system of Fig. 1 has been simulated in the DIgSILENT PowerFactory software. The four-leg VSI is equipped with the suggested control scheme. The types of loads are resistive, and other parameters of the system are presented in Table II. Different simulation case studies under various load scenarios are carried out to determinate the effectiveness of the transient performances of the suggested control scheme.

The evaluation of the transient behavior of the proposed control strategy is made for a three-phase unbalanced load ($R_a = 10\ \Omega,\ R_b = 7\ \Omega,\ R_c = 8\ \Omega$). To verify the transient performance of the proposed voltage control strategy a step change in the d-components of voltage references ($V_{d\,ref}$) in all phases of the four-leg inverter is applied, then back to initial voltage value (while keeping $V_{q\,ref} = 0$).

For the a-phase a step change from 155.56 to 75 V (peak) at 26 ms is applied, then back to initial voltage value at 79 ms. The transient behaviors of the voltage reference ($V_{a,d\ ref}$) and the actual voltage ($V_{a,d}$ ) of the respective phase are shown in Fig. 5. The d-reference voltage (peak) value in phase ‘b’ ($V_{b,d\ ref}$) is step changed from 155.56 to 140 V (peak) at 39 ms, afterwards back to 155.56 V at 79 ms. Fig. 6 also depicts the transient response of the voltage ($V_{b,d\ ref}$) reference and the actual voltage ($V_{b,d}$) of the b-phase.

For the c-phase also a step change from 155.56 to 135 V (peak) at 46 ms is applied, then back to initial voltage value at 79 ms. Fig. 7 illustrates the waveforms of the voltage ($V_{c,d\ ref}$) reference and actual voltage ($V_{c,d}$) of the pertaining phase. As can be seen, the voltage controllers in each phase demonstrate very fast dynamic, and the actual voltages are capable of following closely their references. The PI controllers take about 1 cycle to track its reference in each phase. It is apparent that the proposed controller can be changed the load voltages close to their references with very fast dynamic.

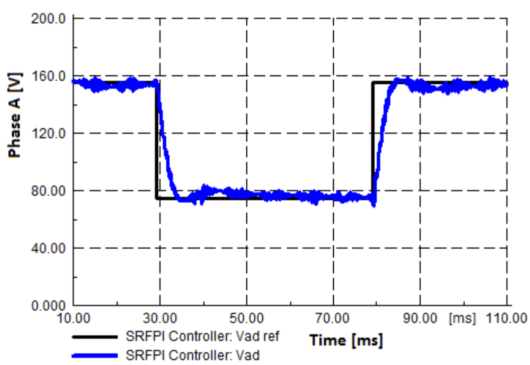


Fig. 5. Transient response of the PI controller to step changes in phase ‘a’.

TABLE II. SYSTEM PARAMETERS FOR THE SIMULATION STUDY.

| | |
|---|---|
| Load voltage | 155.56 V/phase (peak) |
| Frequency | 60 Hz |
| Current controller parameter | K=1 |
| PI voltage controller parameters | $K_p = 0.15, K_I = 42$ |
| Balanced load | $R_A = R_B = R_c = 8\Omega$ |
| Unbalanced loads | $R_a = 10\ \Omega, R_b = 7\ \Omega, R_c = 8\ \Omega$ |
| | $R_a = R_b = 8\Omega, R_c = \infty$ |
| | $R_b = 8\ \Omega, R_a = R_c = \infty$ |

Moreover, the transient performance of the proposed control strategy has been compared with the conventional control scheme [18, 19], with the same specification for the voltage and current controller. In this simulation, while the three-phase four-leg grid-forming unit is initially supplying a balanced load (8 Ω/ph), a single-phase inductive load (R = 20 Ω and L= 2 mH) is added between phases ‘a’ and ‘c’ at 0.3 s. After 0.2 s, the connected load between phase ‘c’ and neutral is changed from the nominal load to a pure resistive of 5.7 Ω. Lastly, the nominal load between phase ‘a’ and neutral is disconnected at 0.7 s.

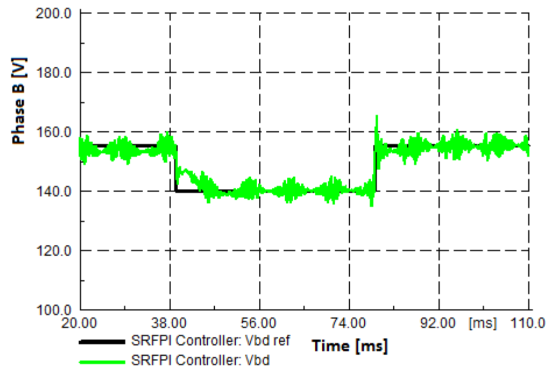


Fig. 6. Transient response of the PI controller to step changes in phase ‘b’.

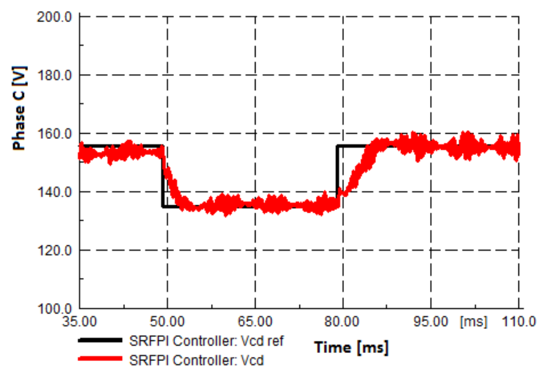


Fig. 7. Transient response of the PI controller to step changes in phase ‘c’.

The output waveforms of load voltages under varying unbalanced load conditions are depicted in Fig. 8, for both the conventional and the suggested control schemes. As can be seen, both control strategies can be remained the load voltages balanced in steady-state under varying unbalanced load conditions. To compare the speed of response of two control schemes, the transient load voltages for both control strategies are provided with zoomed Figures. It can be seen that the load voltage waveforms are unaffected by the load transients in the proposed scheme. Comparing the two results, it can be seen that no significant changes in the load voltages can be observed with the proposed scheme. While there exist at least three line cycles transient with the conventional approach. The results show that the suggested controller has a significant ability to balance the output voltages under severe unbalanced load conditions with zero steady-state error and fast dynamic response.

## V. CONCLUSION

A new per-phase cascaded voltage-current control strategy for a three-phase four-leg VSI operating with highly unbalanced loads in a stand-alone distribution network is presented in this paper. The suggested control scheme provides balanced output voltages for the four-leg inverter even under extremely unbalanced loading conditions. It consists of an outer voltage loop in each phase to regulate the instantaneous output voltages and an inner current loop in each phase to improve the transient behaviors of the control system. The transient performance of the suggested control scheme is investigated using simulation studies. The simulation results show that the suggested controller has a significant ability to balance the output voltages under severe unbalanced load conditions with fast dynamic response.

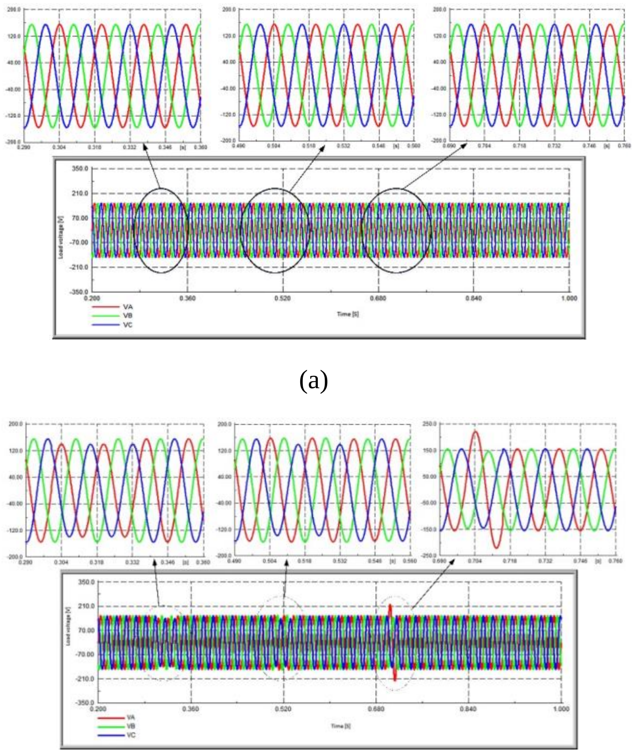

(a)

(b)

Fig. 8. Waveforms of output voltages of the four-leg inverter for different load condition. (a) Proposed control scheme. (b) Conventional scheme [16, 17].

## References


[1] Miveh, M. R., Rahmat, M. F., Mustafa, M. W., & Ghadimi, A. A. (2016). Progress in controlling autonomous microgrids. Electronics World, 122(1957), 20-23.

[2] M. R. Miveh, M. F. Rahmat, M. W. Mustafa, “A new per-phase control scheme for three-phase four-leg grid-connected inverters”, Electronics World, 120(1939), 30-36 (2014).

[3] Miveh, M. R., Rahmat, M. F., Ghadimi, A. A., & Mustafa, M. W. (2016). Control techniques for three-phase four-leg voltage source inverters in autonomous microgrids: A review. Renewable and Sustainable Energy Reviews, 54, 1592-1610.

[4] Miveh, M. R., Rahmat, M. F., Ghadimi, A. A., & Mustafa, M. W. (2015). Power Quality Improvement in Autonomous Microgrids Using Multi-Functional Voltage Source Inverters: A Comprehensive Review. Journal of Power Electronics, 15(4), 1054-1065

[5] Mariam, L., Basu, M., & Conlon, M. F. (2013). A review of existing microgrid architectures. Journal of Engineering, 2013.

[6] S. H. Fathi, H. Rastegar, A. A. Ghadimi, “Control of islanded industrial networks with fuel cell based distributed generation units and ultra-capacitor storage device”, *European Transactions on Electrical Power*, 21(1), 801-823 (2011).

[7] Moghaddam, M. J. H., Bigdeli, M., & Miveh, M. R. (2015). A Review of the Primary-Control Techniques for the Islanded Microgrids/Pregled primarnih krmilnih tehnik za otocne mikromreze. Elektrotehniski Vestnik, 82(4), 169.

[8] Q. C. Zhong and T. Hornik, “Cascaded current–voltage control to improve the power quality for a grid-connected inverter with a local load,” *Industrial Electronics, IEEE Transactions on,* (60)4, 1344-1355 (2013).

[9] Meng, Lexuan, Xin Zhao, Fen Tang, Mehdi Savaghebi, Tomislav Dragicevic, Juan C. Vasquez, and Josep M. Guerrero. "Distributed Voltage Unbalance Compensation in Islanded Microgrids by Using a Dynamic Consensus Algorithm." Power Electronics, IEEE Transactions on 31, no. 1 (2016): 827-838.

[10] R. Omar and N. A. Rahim, “Voltage unbalanced compensation using dynamic voltage restorer based on supercapacitor,” *Int J Electr Power Energy Syst*, 43(1), 573–81(2012).

[11] F. Tang, X. Zhou, L. Meng, J. M. Guerrero, J. C. Vasquez, “Secondary voltage unbalance compensation for three-phase four-wire islanded microgrids,” *Multi-Conference on Systems, Signals & Devices (SSD), 2014 11th International*, 1-5 (2014).

[12] Zhang X, Wang J, Li C. Three-Phase Four-Leg Inverter Based on Voltage Hysteresis Control. IEEE International Conference on Electrical and Control Engineering 2010; 4482-4485.

[13] Li, Y., Vilathgamuwa, D. M., & Loh, P. C. (2005). Microgrid power quality enhancement using a three-phase four-wire grid-interfacing compensator. Industry Applications, IEEE Transactions on, 41(6), 1707-1719.

[14] Li, Y. W., Vilathgamuwa, D. M., & Loh, P. C. (2006). A grid-interfacing power quality compensator for three-phase three-wire microgrid applications. Power Electronics, IEEE Transactions on, 21(4), 1021-1031.

[15] Rokrok E, Hamedani M E. Comprehensive Control Scheme for an Inverter-based Distributed Generation Unit. Iranian Journal of Science & Technology, Transaction B: Engineering 2009; Vol. 33, No. B6, pp 477-490.

[16] Nazifi, H., & Radan, A. (2013, February). Current control assisted and non-ideal Proportional-Resonant voltage controller for four-leg three-phase inverters with time-variant loads. In Power Electronics, Drive Systems and Technologies Conference (PEDSTC), 2013 4th (pp. 355-360). IEEE.

[17] Wang, F., Duarte, J. L., & Hendrix, M. A. (2011). Grid-interfacing converter systems with enhanced voltage quality for microgrid application—concept and implementation. Power Electronics, IEEE Transactions on, 26(12), 3501-3513.

[18] Vechiu I, Camblong H, Tapia G, Dakyo B, Curea O. Control of four leg inverter for hybrid power system applications with unbalanced load. Energy Conversion and Management 2007; 48 2119–2128.

[19] Vechiu, I., Curea, O., & Camblong, H. (2010). Transient operation of a four-leg inverter for autonomous applications with unbalanced load. Power Electronics, IEEE Transactions on, 25(2), 399-407.

[20] Cárdenas R, Peña P, Wheeler P, Clare J, Juri C. Control of a matrix converter for the operation of autonomous systems. Renewable Energy 2012; 43 343-353.

[21] P. Cortes, G. Ortiz, J. Yuz, J. Rodriguez, S. Vazquez, and L. Franquelo, “Model predictive control of an inverter with output LC filter for UPS applications,” IEEE Trans. Ind. Electron., vol. 56, no. 6, pp. 1875–1883, Jun. 2009.

[22] Yaramasu, V., Rivera, M., Narimani, M., Wu, B., & Rodriguez, J. (2014). Model Predictive Approach for a Simple and Effective Load Voltage Control of Four-Leg Inverter with an Output LC Filter.

[23] Yaramasu, V., Rivera, M., Narimani, M., Wu, B., & Rodriguez, J. (2015). High performance operation for a four-leg NPC inverter with two-sample-ahead predictive control strategy. Electric Power Systems Research, 123, 31-39.

[24] Yang, L. Y., Liu, J. H., Wang, C. L., & Du, G. F. (2014). Sliding Mode Control of Three-Phase Four-Leg Inverters via State Feedback. Journal of Power Electronics, 14(5), 1028-1037.

[25] P. Rodriguez, A. Luna, R. S. Munoz-Aguilar, I. Etxeberria-Otadui, R. Teodorescu, F. Blaabjerg,” A stationary reference frame grid synchronization system for three-phase grid-connected power converters under adverse grid conditions,” *Power Electronics, IEEE Transactions on*, 27(1), 99-112 (2012).